Jurnal Elektronika dan Telekomunikasi (JET), Vol. 24, No. 2, December 2024, pp. 105-111
Accredited by KEMDIKBUDRISTEK, Decree No: **158/E/KPT/2021**
doi: 10.55981/jet.635

Compact Dual Port UWB MIMO Antenna with WLAN Band Rejection

Firdaus Firdaus [a, b, *], Intan Aprillia Ikhsan [a], Rahmadi Kurnia [a], Ikhwana Elfitri [a]

[a] *Department of Electrical Engineering*
Andalas University
Kampus Limau Manis
Padang, Indonesia
[b] *Department of Electrical Engineering*
Politeknik Negeri Padang
Kampus Politeknik Negeri Padang Limau Manis
Padang, Indonesia

Abstract

This research presents the design of a compact dual-port ultrawideband multiple input multiple output (UWB MIMO) antenna. The primary challenge in designing UWB MIMO antennas is achieving operation at the low-frequency band of 3.1 GHz while maintaining a small size. By modifying the patch shape to a tapered configuration, incorporating an inset feed, and adding a slit for the wireless local area network (WLAN) notch band, a rectangular monopole patch antenna successfully overcomes these limitations. The MIMO configuration of this antenna achieves a wide UWB bandwidth of 3.1 – 12 GHz with compact dimensions of 20 × 28.5 × 1.6 mm. The antenna exhibits excellent characteristics, including low mutual coupling (-15 dB), maximum gain of 3 dBi, low envelope correlation coefficient (ECC<0.01), high diversity gain (<9.95), low total active reflection coefficient (TARC < -20 dB), and nearly omnidirectional radiation pattern. These results demonstrate the suitability of the proposed antenna design for UWB applications.

Keywords: mutual coupling, UWB, MIMO, band notched, C-slot.

I. INTRODUCTION

Research on ultrawideband (UWB) and multiple input multiple output (MIMO) holds significant importance in advancing wireless communication systems. UWB enables fast and accurate short-range data transfer, while MIMO enhances spectrum efficiency and system reliability through spatial diversity. The integration of UWB and MIMO yields synergies, delivering superior performance and innovative solutions for high-speed wireless communication and high spectrum efficiency. These advancements have a positive impact, especially in applications requiring high-speed, accurate, and reliable wireless data transfer.

Antennas play a pivotal role in UWB MIMO systems. By investigating innovative antenna designs and configurations, such as the monopole patch antenna, we can enhance the overall performance of UWB MIMO systems, contributing to improved spectral efficiency, reduced interference, and enhanced communication capabilities. The monopole patch antenna [1] – [5], a popular choice for UWB systems, consists of a planar radiating element and a partial ground plane, resulting in a compact and simple design with an omnidirectional radiation pattern.

* Corresponding Author.
Email: firdaus @student.unand.ac.id
Received: April 22, 2024 ; Revised: August 06, 2024
Accepted: September 26, 2024 ; Published: December 31, 2024

Interference in the UWB frequency range from technologies such as worldwide interoperability for microwave access (WiMAX) and wireless local area network (WLAN) arises due to overlapping frequency bands. WiMAX and WLAN operate within the UWB spectrum, causing interference that can degrade UWB signal quality. To mitigate this, band-notched UWB antennas are employed, selectively filtering out frequencies associated with WiMAX and WLAN to ensure improved coexistence and minimal interference in UWB communication systems. Various techniques, such as stubs [6], [7], slots [8], [9], slits [10], split ring resonators (SRR) [11], open-loop resonators [12], and electromagnetic band gaps [13], are employed to achieve band notching in antennas. Each method contributes to customizing the antenna's frequency response for specific applications.

A UWB MIMO antenna utilizing a UWB monopole design integrates multiple UWB monopole antennas within the system [14] – [23]. Mutual coupling, or the electromagnetic interaction between adjacent antennas, is a critical consideration in integrating multiple monopole antennas for MIMO. Managing mutual coupling is essential to minimize interference, ensuring each antenna's independence for optimal signal transmission and reception in UWB MIMO systems. This can be achieved by configuring antenna elements orthogonally [17] – [24], complementarily [25] – [30], or incorporating decoupling structures [17] – [19], [24], [31], [32].

The miniaturization of UWB MIMO antennas is essential to meet the demands of increasingly compact mobile devices. However, reducing antenna size presents significant challenges in designing antennas that can effectively cover the low-frequency band of UWB (3.1 – 10.6 GHz) while minimizing mutual coupling between antenna elements. A typical 2 × 2 MIMO system requires two antennas each at the transmitter and receiver. Numerous designs of two-element UWB MIMO antennas with various geometries have been proposed. Table 1 provides a comparative overview of several reported designs, illustrating the trade-offs between antenna size and performance. The physical dimensions of an antenna directly affect its performance. Larger antennas generally offer better coverage of the low-frequency band and reduced mutual coupling.

Unfortunately, miniaturization often leads to a trade-off, resulting in degraded low-frequency performance and increased mutual coupling due to the reduced dimensions and closer proximity of antenna elements.

This paper presents a compact two-port UWB MIMO antenna design. The antenna successfully operates in the typical low-frequency range of UWB through the combination of two patch elements and low mutual coupling. The antenna design is fabricated on a 20 × 28.5 × 1.6 mm flame-retardant 4 (FR-4) substrate with a dielectric constant of 4.4, and the antenna features extremely compact patch elements measuring 3.8 × 8.42 mm and a port-to-port spacing of 16.9 mm. A tapered patch with an inset feed is utilized to enhance impedance matching across the wide frequency band. Furthermore, a C-shaped slot is incorporated into the patch to mitigate performance in the WLAN band. Simulation and measurement results validate the proposed antenna's suitability for UWB MIMO applications.

II. Antenna Design

A. Antenna Structure

The antenna structure in this paper, as illustrated in Figure 1, consists of two rectangular-shaped monopole elements with a tapered lower side and a common ground. Both of these antenna elements have identical dimensions. The complete dimensions of the antenna are 20 × 28.5 mm, which is equivalent to a wavelength of $0.2\lambda_o \times 0.28\lambda_o$. λ_o represents the wavelength in free space at the initial resonance frequency of approximately 3.0 GHz. Nevertheless, the primary objective of this antenna research is to achieve a minimum operating frequency of 3.1 GHz while maintaining a compact size. The initial stages of antenna design involve carefully selecting antenna geometry and parameters to meet the specific required operating frequency. In pursuit of a miniaturized UWB antenna design, a monopole structure is chosen, and the estimated lowest frequency range of the selected monopole can be determined according to the formula by [33], as written in (1).

$$fr = \frac{14.4}{l_1 + l_2 + g + \frac{A_1}{2\pi\sqrt{\epsilon_r + 1}} + \frac{A_2}{2\pi\sqrt{\epsilon_r + 1}}} \quad (1)$$

A_1 indicates the ground plane region, while A_2 represents the combined ground plane and radiation patch region. Similarly, l_1 represents the ground plane length and l_2 represents the radiator monopole length. The gap between the ground area and the radiator is denoted by g. All dimensions (A_1, A_2, l_1, l_2, and g) are in millimeters.

The monopole patch is configured in a rectangular shape with dimensions $l \times j$, and subsequently extended to incorporate a tapered lower side with a length of m. The connection of the monopole antenna is established on the lower side of the monopole patch using a microstrip line with dimensions $l \times k$. To improve impedance matching at lower frequencies, an inset feed is introduced at the junction of the monopole patch and microstrip line. A C-shaped slot is also cut onto the patch to create a notched band at WLAN frequencies. The optimized design of the proposed antenna is shown in Table 2. The UWB MIMO antenna is built on an FR4

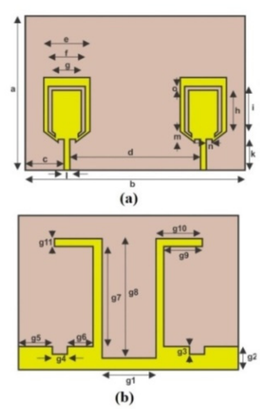

Figure 1. The shape of the designed UWB MIMO antenna.

TABLE 1
TWO-PORT UWB MIMO ANTENNA COMPARISON

Reference #	Overall Size (mm × mm)	Port distance	Radiator size	S_{11}	Isolation (dB)	Band Notched (GHz)	Gain (dBi)	efficiency	ECC
[34]	21 × 30	22	r = 22	2.14 – 11.4	– 20	-	6.5	55% - 88%	0.25
[35]	35 × 50	48	r = 9.1	3 – 11	– 25	-	3	80%	0.004
[36]	29 × 50	20	16 × 50	2.4 – 11	– 20	-	2.5	60%	0.04
[37]	120 × 60	56	16 × 50	1 – 4.5	– 12.5	-	3.98	92.5%	0.19
[24]	22 × 31	11	7.34 × 8	2.9 – 12	– 15	-	2.31	-	0.3
[17]	18 × 34	19.3	55 × 7.35	2.9 – 20	– 22	5.1 – 5.8 & 6.7 – 71	7	85%	0.01
[18]	50 × 30	18	15 × 15	2.5 – 14	– 20	-	4.3	-	0.04
[19]	30 × 40	17	11.2 × 12	3.1 – 10.6	-	3.4 – 3.7 & 5.15 – 5.35	4	80%	-
[31]	22 × 36	20	8 × 8	3.1 – 11	– 15	1.15 – 5.18	4	80%	0.1
[38]	35 × 35	28	7.5 × 9	2 – 12	–20	5.15 – 5.825	-	-	0.3
[21]	32 × 32	20	7 × 8	3.1 – 10.6	–15		4.2	60%	0.02
This Work	20 × 28.5	17.7	7.5 × 3	3.1 – 12	–15	5.3 – 6	3	80%	0.04

substrate that is 0.8 millimeters thick, has a relative permittivity of 4.4, and a loss tangent of 0.02.

The evolution of UWB antenna geometry modifications for achieving the UWB band (3.1 – 10.6 GHz as defined by the FCC) is depicted in Figure 2, with corresponding changes in S_{11} parameters shown in Figure 3. Each stage progressively refines the antenna design. Step 1 utilizes a patch monopole and partial ground plane, resulting in a broad bandwidth (5.96 GHz – 9.28 GHz) but falling short of the full UWB range. Step 2 introduces an inset feed to improve performance, increasing bandwidth to 4 GHz (5.96 GHz – 9.96 GHz) and significantly enhancing impedance matching (minimum reflection of -22 dB at 7.3 GHz), as shown in Figure 3. Step 3 tapers the lower side of the patch, further expanding the bandwidth beyond 12 GHz (evident in Figure 3, where the S_{11} curve dips below -10 dB from 5.8 GHz onwards). The antenna progressively approaches the desired UWB bandwidth requirements through these iterative modifications. Step 4 involves integrating a rectangular slot into the ground plane. This slot has dimensions of $g_3 \times g_4$ mm. This modification enhances impedance bandwidth at higher frequencies, extending up to 14 GHz (not depicted in Figure 3 for visual consistency, as it is limited to 12 GHz). To achieve a more consistent impedance bandwidth for UWB, a flipped L-shaped stub is introduced to the ground as in Step 5. The outcome is a stable S_{11} curve below -10 dB, although further adjustments are still necessary for lower frequencies.

In order to suppress WLAN interference, a slot in C form is added to the patch monopole as illustrated in Step 5. By adding this component, the UWB antenna can now operate at 3.1 GHz and effectively blocks WLAN signals between 5.3 and 6 GHz. However, performance in the 3.4 – 4.8 GHz range still requires enhancement.

Finally, the antennas in Step 6 are combined to form an antenna in MIMO configuration. The antenna meets the lower frequency requirement of 3.1 GHz and exhibits a notched band at frequencies 5.3 – 6 GHz (WLAN). Excellent isolation between antenna elements is achieved, as illustrated in Figure 4, where S_{12} is below -20 dB across all of the UWB working frequencies.

B. Influence of the Decoupling Structure

The proposed antenna boasts improved impedance matching and enhanced isolation thanks to the decoupling structure, leading to significantly enhanced performance. Figure 5 depicts the sequential progression in refining the ground plane design as the decoupling structure for the antenna. For identical UWB MIMO antenna elements, the value of S_{11} will be similar to S_{22}, and S_{12} will be similar to S_{21}. Therefore, only S_{11} and S_{12} are shown in Figure 5. Figure 5(a) shows the formation of a MIMO antenna by combining UWB antenna elements with a partial ground area. The antenna exhibits poor performance because it does not reach low frequencies, and the isolation among its elements is poor. Figure 5(a) shows that S_{11} for ground without connection. It has a lower frequency of 5.1 GHz ($S_{11} < -10$), while UWB requires 3.1 GHz. The S_{12} parameter curves in Figure 5(a) show insufficient isolation between the antennas, which exceeds the intended threshold of -20 dB.

Connecting the two partial ground planes in Figure 5(b) significantly enhances antenna-to-antenna isolation in the 4 – 5 GHz range, exceeding the desired -20 dB threshold. However, isolation falls short in the 2 – 4 GHz and 6 – 12 GHz ranges. Adding vertical microstrip lines, as depicted in Figure 5(c), further improves isolation above – 10 dB within the 4 – 12 GHz range. Adding a

TABLE 2
DIMENSIONS OF THE DESIGNED UWB MIMO ANTENNA

Parameters	a	B	C	D	e	F	g
Unit (mm)	20	28.5	5.02	16.9	6	4.8	3.8
Parameters	**h**	**I**	**J**	**K**	**l**	**M**	**n**
Unit (mm)	5.35	5.85	7	4	0.76	1.42	0.75
Parameters	**o**	**g1**	**g2**	**g3**	**g4**	**g5**	**g6**
Unit (mm)	0.5	7	3	1	2	4.37	3.37
Parameters	**g7**	**g8**	**g9**	**g10**	**g11**		
Unit (mm)	13	15.5	5	6	1		

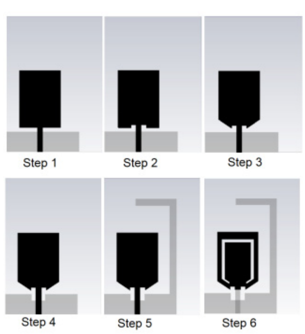

Figure 2. UWB antenna step design.

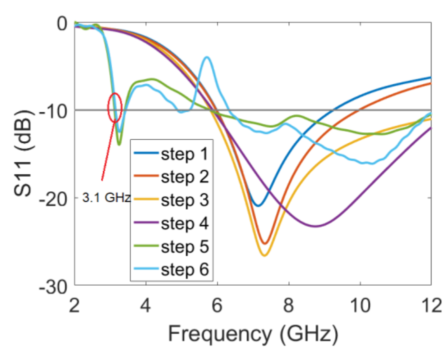

Figure 3. S_{11} of geometry step.

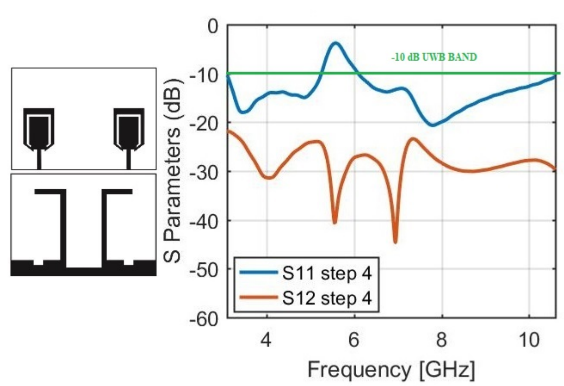

Figure 4. UWB MIMO antenna.

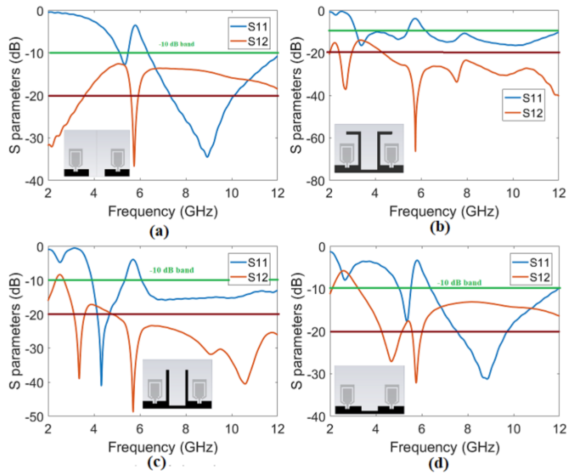

Figure 5. Development of the ground plane geometry.

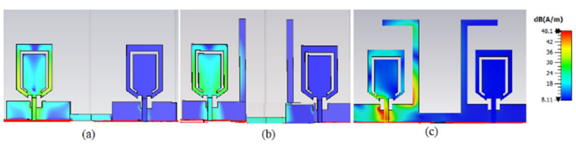

Figure 6. Current distribution of ground evolution.

horizontal strip to the existing structure, forming an inverted-L pattern, significantly enhances isolation. With this new configuration, we successfully achieved an optimal low frequency of up to 3.1 GHz, fulfilling the requirements for UWB applications (Figure 5(d)). These features lower the resonance and cutoff frequencies to 3.4 GHz and 3.1 GHz, respectively, and suppress coupling throughout the 3.1 – 12 GHz band, achieving an isolation below -22 dB, meeting the required isolation threshold for optimal MIMO performance.

Figure 6 demonstrates the effectiveness of decoupling structures in enhancing isolation between antenna elements. Without L-stubs (Figure 6(a)), when one port is excited and the other is terminated, current still flows through the terminated port. Adding an I-stub (Figure 6(b)) reduces the surface current at the terminated port but does not completely eliminate it, leading to insufficient isolation. By employing a reverse L-stub instead (Figure 6(c)), isolation improves significantly to more than -20 dB across the entire 3.1 – 12 GHz band, except for the WLAN band.

C. Influence of C-Slot

The notched band WLAN characteristic of the proposed UWB MIMO antenna was obtained using C-slots on each antenna element. The C-slots caused a mismatch condition between the feed line and the antenna element at the 5.3 – 6 GHz band, so the notched band characteristic is obtained. The influence of the C-slot can also be seen by displaying the surface current vector at a frequency of 5.7 GHz to obtain a WLAN band rejector. Figure 7 clearly shows the surface current pattern, with a high concentration around the C-slot. The currents in the two arms have opposite phases and thus cancel each other, contributing to the band rejection characteristic. Therefore, the radiation from the current

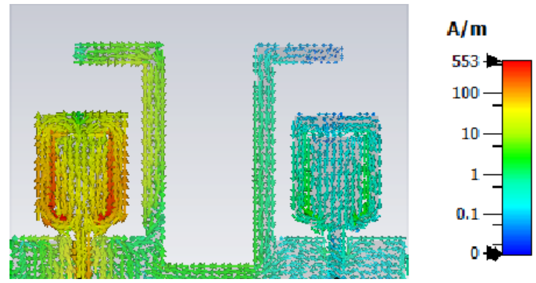

Figure 7. Current distribution of C-slot.

in one arm of the C-slot is canceled by the current in the other arm, resulting in minimal radiation at the 5.8 GHz WLAN band. This contributes to the high return loss, indicating efficient cancellation of unwanted radiation and the effectiveness of the designed antenna in providing a band-cancelation characteristic at the WLAN frequency.

III. Result and Discussion

The final UWB MIMO antenna design is printed on a FR-4 substrate with a dielectric constant (ε_r) of 4.4 and a loss tangent (tanδ) of 0.025, with dimensions of 20 × 28.5 × 1.6 mm, as depicted in Figure 8. The Keysight E5071C Vector Network Analyzer has been utilized to evaluate predicted and measured findings for the designed antenna, focusing on return loss, radiation pattern, MIMO diversity, and gain. This verification is critical to ensure the accuracy and efficacy of the antenna design, as well as validate its performance prior to practical implementation.

Figure 9 shows a comparison between simulation and measurement results for S_{11} and S_{12}. The measurements correlate well with the simulated results.

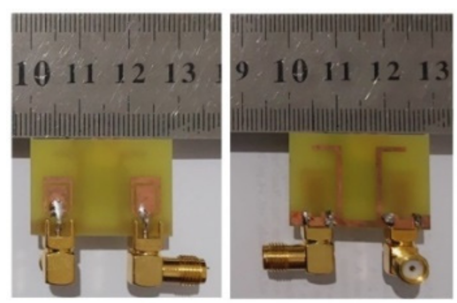

Figure 8. Antenna realization.

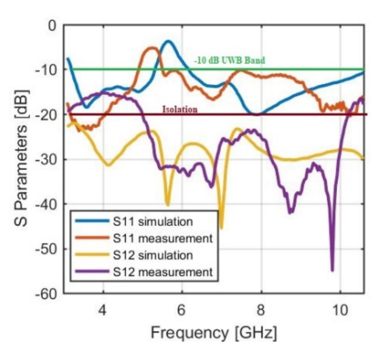

Figure 9. Predicted and measured reflection coefficients.

The S_{11} value is less than -10 dB for 3.1 GHz to over 12 GHz. A frequency band notch is created in the 5.3 – 6 GHz frequency band, which is suitable for avoiding interference from WLAN. S_{12} is below -20 dB for frequencies of 5.5 – 10.1 GHz but exceeds -15 dB in the 3 – 5.5 GHz. Furthermore, the S_{12} parameter reveals excellent isolation properties within the 5.5 – 10.1 GHz band; however, it exhibits a decline in isolation within the 3 – 5.5 GHz range. Nevertheless, it is still sufficient for MIMO systems where S_{11} is below -10 dB, and S_{12} is below -15 dB.

The antenna gain realization is shown in Figure 10. The gain varies between 0 and 3 dBi across the UWB band. In the 5.3 – 6 GHz cancellation band, the antenna gain drops sharply to -4 dB, demonstrating the antenna's ability to suppress the notch band frequency. The simulation results closely match the measurements. Figure 11 compares the predicted and measured antenna patterns at 3.1, 5, and 10 GHz in the E-plane and H-plane. The antenna exhibits a near-omnidirectional radiation pattern across the UWB operating band, although there are slight differences between the predicted and measured results.

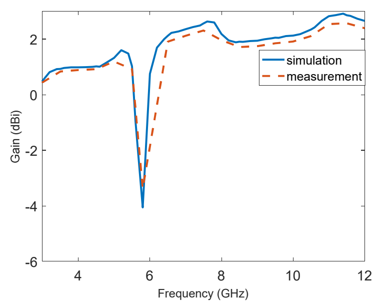

Figure 10. The gain realization of the proposed antenna.

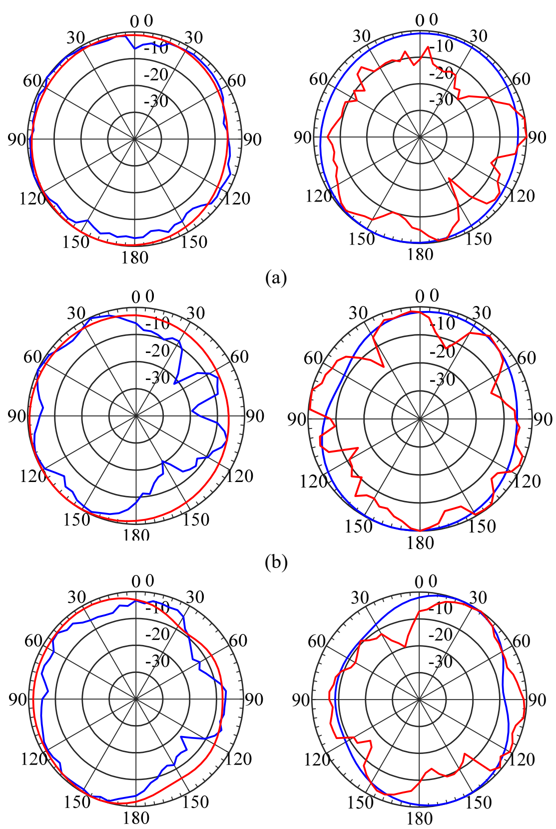

(a)

(b)

(c)

Figure 11. Radiation pattern performance of proposed antenna at (a) 3.1 GHz, (b) 5 GHz, and (c) 10 GHz. (left side = E-plane, right size = H-plane).

IV. MIMO PERFORMANCE

UWB MIMO antenna performance is evaluated using several parameters. The envelope correlation coefficient (ECC) measures the correlation between the signals received by the MIMO antenna elements. ECC is a metric that indicates the degree of independence between the fading channels experienced by different antennas. A low ECC value is desirable, indicating independent fading across the elements, which maximizes spatial diversity gain. Conversely, a high ECC value indicates a strong signal correlation, which can degrade system performance. ECC is given mathematically by [33], as described in (2).

$$ECC = \frac{|S_{11}^{*}S_{12}+S_{21}^{*}S_{22}|}{(1-(|S_{11}|^2+|S_{21}|^2))(1-(|S_{22}|^2+|S_{12}|^2))} \qquad (2)$$

Ideally, for an uncorrelated diversity antenna, the ECC should be zero. However, realistically, values below 0.5 are deemed satisfactory. Our proposed UWB MIMO/diversity antenna demonstrates exceptionally low ECC, as evidenced in Figure 12 by both simulated and measured curves. Notably, the calculated ECC based on S-parameters for this design is remarkably low at less than 0.01. Diversity gain (DG) measures the improvement in signal-to-noise ratio (SNR) achieved by using a MIMO antenna system compared to a single antenna. High diversity gain indicates significant performance improvement in multipath environments. To calculate the DG of the designed UWB MIMO antenna, we use the formula by [15], as written in (3).

$$DG = 10\sqrt{1-ECC}. \qquad (3)$$

As presented in Figure 13, the proposed antenna has an impressively low ECC (<0.01) and a significantly high DG (>9.95 dB), both calculated using S-parameters, demonstrating its exceptional antenna performance. Total active reflection coefficient (TARC) measures the amount of signal reflection from the antenna back to the transmitter. A low TARC value indicates high antenna efficiency, while a high TARC value indicates significant power loss due to reflection. For the 2 × 2 MIMO system, the TARC formula follows [26], as described in (4).

$$\Gamma_a^t = \sqrt{\frac{\left(\left(|S_{11}+S_{12}e^{j\theta}|^2\right)+\left(|S_{22}+S_{21}e^{j\theta}|^2\right)\right)}{2}} \qquad (4)$$

Minimizing TARC is critical for maximizing the isolation of MIMO antennas. As illustrated in Figure 13, both measured and simulated TARC values below -20 dB

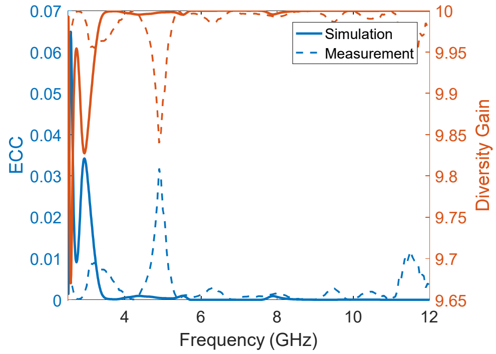

Figure 12. ECC and Diversity Gain of the proposed antenna.

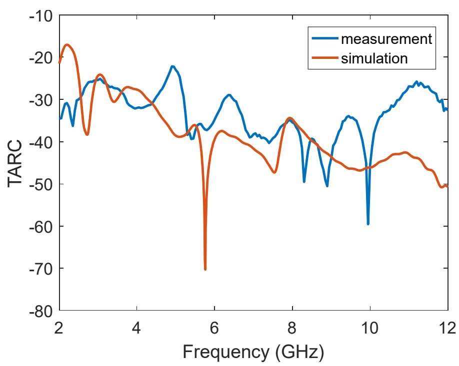

Figure 13. TARC comparison of the proposed antenna.

across the entire operational band exceeded the desired performance benchmarks for MIMO systems.

Table 2 showcases the extent of size reduction achieved by our proposed antenna compared to similar designs from recent literature. The comparison highlights notable miniaturization in terms of both physical dimensions and performance characteristics.

V. Conclusion

A compact MIMO UWB antenna with dimensions of 20 × 28.5 × 1.6 mm has been successfully designed and fabricated. The antenna exhibits a wide operating bandwidth from 3.1 to 12 GHz, with isolation better than -20 dB across most of the band and exceeding -15 dB in the lower frequency (3.1 – 4.8 GHz). The antenna also effectively suppresses WLAN interference in the 5.3 – 6 GHz band. The maximum gain achieved is 3 dBi, while the ECC < 0.01. The diversity gain is as high as 9.95, and the TARC is below -20 dB. Furthermore, the antenna exhibits a nearly omnidirectional radiation pattern, ensuring reliable coverage in various environments. Based on these comprehensive performance metrics, the proposed antenna emerges as a promising candidate for integration into portable UWB communication devices.

Declarations

Conflict of Interest

We, the authors, declare that this research is free from any conflicts of interest. Our work has not been influenced by financial, professional, or personal relationships.

CRediT Authorship Contribution

Firdaus: Conceptualization, Methodology, Investigation, Validation, Writing-Original Draft; Intan Aprillia Ikhsan: Conceptualization, Investigation, Validation; Rahmadi Kurnia: Supervision, Writing-Reviewing and Editing; Ikhwana Elfitri: Conceptualization, Supervision, Writing-Reviewing and Editing.

Funding

Research reported in this publication was supported by the Ministry of Education, Culture, Research, and Technology of the Republic of Indonesia through the Research and Development Allocation Fund (DIPA) Politeknik Negeri Padang under grant number 176/PL9.15/PG/2023.

Acknowledgment

We would like to express our sincere gratitude to the Antenna and Propagation Laboratory of Universitas Andalas and Politeknik Negeri Padang for providing the necessary facilities and resources to conduct this research. Their support and assistance were invaluable to the completion of this project.

References

[1] H. Mardani, C. Ghobadi, and J. Nourinia, "A simple compact monopole antenna with variable single- and double-filtering function for uwb applications," *IEEE Antennas Wirel. Propag. Lett.*, vol. 9, pp. 1076–1079, 2010, doi: 10.1109/LAWP.2010.2091391.

[2] O. M. H. Ahmed, A. R. Sebak, and T. A. Denidni, "Compact UWB printed monopole loaded with dielectric resonator antenna," *Electron. Lett.*, vol. 47, no. 1, pp. 7–8, 2011, doi: 10.1049/el.2010.7337.

[3] Z. L. Zhou, L. Li, and J. S. Hong, "Compact UWB printed monopole antenna with dual narrow band notches for WIMAX/WLAN bands," *Electron. Lett.*, vol. 47, no. 20, p. 1111, 2011, doi: 10.1049/el.2011.2299.

[4] N. Ojaroudi, M. Ojaroudi, and N. Ghadimi, "UWB omnidirectional square monopole antenna for use in circular cylindrical microwave," *IEEE Antennas Wirel. Propag. Lett.,* vol. 11, pp. 1350–1353, 2012, doi: 10.1109/LAWP.2012.2227137.

[5] J. Y. Siddiqui, C. Saha, and Y. M. M. Antar, "Compact SRR loaded UWB circular monopole antenna with frequency notch characteristics," *IEEE Trans. Antennas Propag.*, vol. 62, no. 8, pp. 4015–4020, 2014, doi: 10.1109/TAP.2014.2327124.

[6] H. Hosseini, H. R. Hassani, and M. H. Amini, "Miniaturised multiple notched omnidirectional UWB monopole antenna," *Electron. Lett.*, vol. 54, no. 8, pp. 472–474, 2018, doi: 10.1049/el.2017.4528.

[7] M. Abdollahvand, G. Dadashzadeh, and D. Mostafa, "Compact dual band-notched printed monopole antenna for UWB application," *IEEE Antennas Wirel. Propag. Lett.,* vol. 9, pp. 1148–1151, 2010, doi: 10.1109/LAWP.2010.2091250.

[8] E. Antonino-daviu, M. Cabedo-fabrés, M. Ferrando-bataller, V. Miquel, and R. Peñarrocha, "Modal analysis and design of band-notched UWB planar monopole antennas," *IEEE Trans. Antennas Propag.*, vol. 58, no. 5, pp. 1457–1467, 2010, doi: 10.1109/TAP.2010.2044323.

[9] K. Zhang, Y. Li, and Y. Long, "Band-notched UWB printed monopole antenna with a novel segmented circular patch," *IEEE Antennas Wirel. Propag. Lett.,* vol. 9, pp. 1209–1212, 2010, doi: 10.1109/LAWP.2010.2099095.

[10] N. Tasouji, J. Nourinia, C. Ghobadi, and F. To, "A novel printed UWB slot antenna with reconfigurable band-notch characteristics," *IEEE Antennas Wirel. Propag. Lett.,* vol. 12, pp. 922–925, 2013, doi: 10.1109/LAWP.2013.2273452.

[11] O. A. Safia, M. Nedil, L. Talbi, and K. Hettak, "Coplanar waveguide-fed rose-curve shape UWB monopole antenna with dual-notch characteristics," *IET Microwaves, Antennas Propag.*, vol. 12, no.7, pp. 1112–1119, 2018, doi: 10.1049/iet-map.2017.0852.

[12] J. R. Kelly, P. S. Hall, and P. Gardner, "Band-notched UWB antenna incorporating a microstrip open-loop resonator," *IEEE Trans. Antennas Propag.,* vol. 59, no. 8, pp. 3045–3048, 2011, doi: 10.1109/TAP.2011.2152326.

[13] M. Yazdi and N. Komjani, “Design of a band-notched UWB monopole antenna by means of an EBG structure,” *IEEE Antennas Wirel. Propag. Lett.,* vol. 10, pp. 170–173, 2011, doi: 10.1109/LAWP.2011.2116150.

[14] S. Jayant, G. Srivastava, and M. Khari, “8-port MIMO antenna having two notched bands for chipless UWB-RFID tags,” *IEEE J. Radio Freq. Identification,* vol. 6, pp. 355–360, 2022, doi: 10.1109/JRFID.2022.3180196.

[15] Z. Tang, X. Wu, J. Zhan, S. Hu, Z. Xi, and Y. Liu, “Compact UWB-MIMO antenna with high isolation and triple band-notched characteristics,” *IEEE Access*, vol. 7, pp. 19856–19865, 2019, doi: 10.1109/ACCESS.2019.2897170.

[16] B. Yang, M. Chen, and L. Li, “Design of a four-element WLAN/LTE/UWB MIMO antenna using half-slot structure,” *AEU - Int. J. Electron. Commun.*, vol. 93, pp. 354–359, 2018, doi: 10.1016/j.aeue.2018.05.034.

[17] R. Chandel, A. K. Gautam, and K. Rambabu, “Tapered fed compact UWB MIMO-diversity antenna with dual band-notched characteristics,” *IEEE Trans. Antennas Propag.*, vol. 66, no. 4, pp. 1677–1684, 2018, doi: 10.1109/TAP.2018.2803134.

[18] A. Iqbal, O. A. Saraereh, A. W. Ahmad, and S. Bashir, “Mutual coupling reduction using f-shaped stubs in UWB-MIMO antenna,” *IEEE Access*, vol. 6, pp. 2755–2759, 2017, doi: 10.1109/ACCESS.2017.2785232.

[19] T. C. Tang and K. H. Lin, “An ultrawideband MIMO antenna with dual band-notched function,” *IEEE Antennas Wirel. Propag. Lett.*, vol. 13, pp. 1076–1079, 2014, doi: 10.1109/LAWP.2014.2329496.

[20] J. Zhu, B. Feng, B. Peng, L. Deng, and S. Li, “A dual notched band mimo slot antenna system with y-shaped defected ground structure for UWB applications,” *Microw. Opt. Technol. Lett.,* vol. 58, no. 3, pp. 626-630, 2016, doi: 10.1002/mop.29632.

[21] J. Ren, W. Hu, Y. Yin, and R. Fan, “Compact printed MIMO antenna for UWB applications,” *IEEE Antennas Wirel. Propag. Lett.*, vol. 13, pp. 1517–1520, 2014, doi: 10.1109/LAWP.2014.2343454.

[22] L. Liu, S. W. Cheung, and T. I. Yuk, “Compact MIMO antenna for portable UWB applications with band-notched characteristic,” *IEEE Trans. Antennas Propag.*, vol. 63, no. 5, pp. 1917–1924, 2015, doi: 10.1109/TAP.2015.2406892.

[23] W. T. Li, Y. Q. Hei, H. Subbaraman, X. W. Shi, and R. T. Chen, “Novel printed filtenna with dual notches and good out-of-band characteristics for UWB-MIMO applications,” *IEEE Microw. Wireless Components Lett.,* vol. 26, no. 10, pp. 765–767, 2016, doi: 10.1109/LMWC.2016.2601298.

[24] W. Li, Y. Hei, P. M. Grubb, X. Shi, and R. T. Chen, “Compact inkjet-printed flexible MIMO antenna for UWB applications,” *IEEE Access*, vol. 6, pp. 50290–50298, 2018, doi: 10.1109/ACCESS.2018.2868707.

[25] T. K. Roshna, U. Deepak, V. R. Sajitha, K. Vasudevan, and P. Mohanan, “A compact UWB MIMO antenna with reflector to enhance isolation,” *IEEE Trans. Antennas Propag.*, vol. 63, no. 4, pp. 1873–1877, 2015, doi: 10.1109/TAP.2015.2398455.

[26] J. Y. Deng, L. X. Guo, and X. L. Liu, “An ultrawideband MIMO antenna with a high isolation,” *IEEE Antennas Wirel. Propag. Lett.*, vol. 15, pp. 182–185, 2016, doi: 10.1109/LAWP.2015.2437713.

[27] S. K. Dhar, M. S. Sharawi, O. Hammi, and F. M. Ghannouchi, “An active integrated ultra-wideband MIMO antenna,” *IEEE Trans. Antennas Propag.*, vol. 64, no. 4, pp. 1573–1578, 2016, doi: 10.1109/TAP.2016.2537379.

[28] X. T. Yuan, Z. Chen, T. Gu, and T. Yuan, “A wideband PIFA-pair-based MIMO antenna for 5G smartphones,” *IEEE Antennas Wirel. Propag. Lett.*, vol. 20, no. 3, pp. 371–375, 2021, doi: 10.1109/LAWP.2021.3050337.

[29] X. Zhang, Y. Li, W. Wang, and W. Shen, “Ultra-wideband 8-port MIMO antenna array for 5G metal-frame smartphones,” *IEEE Access*, vol. 7, pp. 72273–72282, 2019, doi: 10.1109/ACCESS.2019.2919622.

[30] J. Li, Q. Chu, Z. Li, and X. Xia, “Compact dual band-notched UWB MIMO antenna with high isolation,” *IEEE Trans. Antennas Propag.,* vol. 61, no. 9, pp. 4759–4766, 2013, doi: 10.1109/TAP.2013.2267653.

[31] L. Liu, S. W. Cheung, and T. I. Yuk, “Compact MIMO antenna for portable UWB applications with band-notched characteristic,” *IEEE Trans. Antennas Propag.*, vol. 63, no. 5, pp. 1917–1924, 2015, doi: 10.1109/TAP.2015.2406892.

[32] L. Kang, H. Li, X. Wang, and X. Shi, “Compact offset microstrip-fed MIMO antenna for band-notched UWB applications,” *IEEE Antennas Wirel. Propag. Lett.,* vol. 14, pp. 1754–1757, 2015, doi: 10.1109/LAWP.2015.2422571.

[33] R. Chandel, A. K. Gautam, and K. Rambabu, “Tapered fed compact UWB MIMO-diversity antenna with dual band-notched characteristics,” *IEEE Trans. Antennas Propag.*, vol. 66, no. 4, pp. 1677–1684, 2018, doi: 10.1109/TAP.2018.2803134.

[34] X. L. Liu, Z. D. Wang, Y. Z. Yin, J. Ren, and J. J. Wu, “A compact ultrawideband MIMO antenna using QSCA for high isolation,” *IEEE Antennas Wirel. Propag. Lett.*, vol. 13, pp. 1497–1500, 2014, doi: 10.1109/LAWP.2014.2340395.

[35] L. Wang, Z. Du, H. Yang, R. Ma, Y. Zhao, and X. CuiL, “Compact UWB MIMO antenna with high isolation using fence-type decoupling structure,” *IEEE Antennas Wirel. Propag. Lett.*, vol. 18, no. 8, pp. 1641–1645, 2019, doi: 10.1109/LAWP.2019.2925857.

[36] D. Potti, Y. Tusharika, M. G. N. Alsath, S. Kirubaveni, M. Kanagasabai, and R. Sankararajan, “A novel optically transparent UWB antenna for automotive MIMO communications,” *IEEE Trans. Antennas Propag.*, vol. 69, no. 7, pp. 3821–3828, 2021, doi: 10.1109/TAP.2020.3044383.

[37] X. Zhao, S. Riaz, and S. Geng, “A reconfigurable MIMO/UWB mimo antenna for cognitive radio applications,” *IEEE Access*, vol. 7, pp. 46739–46747, 2019, doi: 10.1109/ACCESS.2019.2909810.

[38] J. Zhu, S. Li, B. Feng, L. Deng, and S. Yin, “Compact dual-polarized UWB quasi-self-complementary MIMO/diversity antenna with band-rejection capability,” *IEEE Antennas Wirel. Propag. Lett.,* vol. 15, pp. 905–908, 2016, doi: 10.1109/LAWP.2015.2479622.